



TITLE:

# Two Dimensional Analysis of MHD Generator by Means of Equivalent Circuit

AUTHOR(S):

YOSHIDA, Masaharu; UMOTO, Jūrō

---

CITATION:

YOSHIDA, Masaharu ...[et al]. Two Dimensional Analysis of MHD Generator by Means of Equivalent Circuit. *Memoirs of the Faculty of Engineering, Kyoto University* 1975, 36(4): 427-442

ISSUE DATE:

1975-03-25

URL:

<http://hdl.handle.net/2433/280960>

RIGHT:

## Two Dimensional Analysis of MHD Generator by Means of Equivalent Circuit

By

Masaharu YOSHIDA\* and Jūrō UMO\*<sup>†</sup>

(Received June 29, 1974)

### Abstract

The authors report on the method analyzing generally the MHD generator by means of the equivalent circuit including the negative resistance. At first, they divide the duct space into many space elements, and for each space element they derive the fundamental equivalent four-terminal circuit which satisfies the two-dimensional Ohm's law. Next, they make an attempt to apply the equivalent circuits to the typical MHD generators such as diagonal, Faraday and Hall generators considering the boundary layer in the duct and the wall leakage current. Using their analysis, the current density, Joule's heat, generated and output electrical powers, electrical efficiency etc. in the generator can be fairly easily calculated.

### 1. Introduction

The fluid performance in MHD generator ducts has been mainly analyzed by the quasi one-dimensional MHD equations for simplification. For the last few years the authors, too, have discussed the optimization of the generator duct on the basis of the quasi one-dimensional MHD equations, and have investigated the influence of boundary layer, finitely segmented electrodes etc. on the generator performance. However, it is difficult to deal accurately with the problem of plasma non-uniformity in the duct cross-section by the above mentioned method.

On the other hand, considering the imperfection of the quasi one-dimensional analysis, the two- or three-dimensional analysis are done, too, by several researchers. In this analysis, they solve numerically the two- or three-dimensional partial differential equations derived from the Maxwell equations and Ohm's law, or do directly and numerically the two- or three-dimensional MHD equations.

Also as another two-dimensional analysis, there is the one using an appropriate equivalent circuit for the generator, which Shirakata<sup>1)</sup>, Celinski<sup>2)~4)</sup> and others derived. For example, Shirakata studied the duct performance in a Faraday

---

\* Department of Electrical Engineering

generator with the four-terminal network. According to his theory, a Faraday duct can be replaced by an equivalent four-terminal network deduced from the two-dimensional Ohm's law in the  $x$ - $y$  plane. His theory also can deal with the problem of nonequilibrium generator considering ionization instability, if it is assumed that the relaxation time of the electron temperature is sufficiently short and all the parameters in the duct are periodical along the flow.

Hence, in this paper, the authors generalize Shirakata's theory and develop it to the generator whose pair of electrodes is slanted. Their theory can be easily applied to the typical MHD generators such as Faraday, Hall and diagonal generators. According to their theory, the generators are quite accurately simulated by means of a four-terminal network, when the duct type and scale, and the temperature and pressure profiles along the gas flow are given.

Moreover, in their analysis, the effects of the boundary layer and wall-leakage currents are considered, but the ion slip is ignored.

## 2. Types of MHD Generator Ducts and Connection of Electrodes and Loads

First, let us pay attention to an MHD duct in which each pair of electrodes is set up at some slant angle to the direction of gas flow, as shown in Fig. 1. When the slant angle  $\theta$  is appropriately selected and the load is appropriately connected, any typical generator duct is obtained as described below.

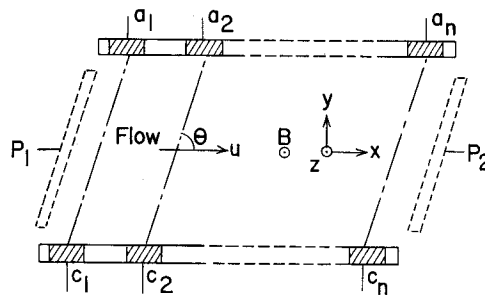


Fig. 1. General form of MHD generator duct (type I).

In the following sections, the authors divide the duct space in Fig. 1 into many space elements, in which all physical quantities may be assumed to be uniform, and derive the fundamental electrical equivalent circuit for the element, and eventually the equivalent network of the whole duct.

Moreover, they apply their equivalent circuit to the typical generators such as Faraday, Hall and diagonal generators, and derive a theoretical calculation of

them. In their application, these three kinds of generators are as follows:

(a) Faraday generator; in Fig. 1, the slope angle  $\theta = \pi/2$  and the load resistances are connected between each pair of electrodes  $a_i$  and  $c_i$  ( $i=1, 2, \dots, n$ ) respectively.

(b) Hall generator; the angle  $\theta = \pi/2$ , each pair of electrodes  $a_i$  and  $c_i$  is shorted respectively, and only a single load resistance is connected between the two electrodes at the inlet and the outlet of the duct.

(c) Diagonal generator; the angle  $\theta$  is set up as an appropriate value ( $0 < \theta < \pi/2$ , if the magnetic field  $B$  is parallel to the  $z$ -axis), and the other conditions are the same as those in the Hall duct. In this connection, the so-called diagonally connected generator duct such as shown in Fig. 2 (type II), in which each pair of Faraday generator electrodes is connected in series, is also known. To this type of duct, too, our analysis for the so-called diagonal conducting wall generator duct of type I in Fig. 1 can be applicable.

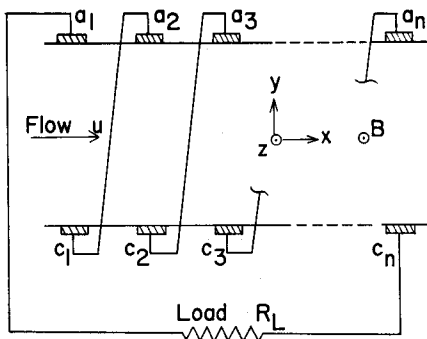


Fig. 2. Diagonally connected generator (type II).

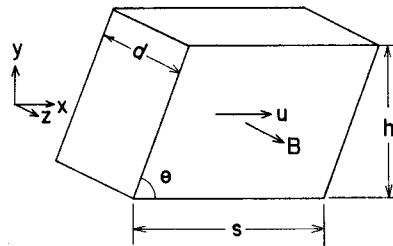


Fig. 3. A space element.

### 3. Derivation of Fundamental Equivalent Circuit

#### 3.1 Equivalent impedance matrix

Fig. 3 shows a space element of the MHD generator duct space which is shown in Fig. 1. Let us try to derive the equivalent four-terminal circuit for the space element from the two dimensional Ohm's law. In the space element, it is assumed that the gas dynamical parameters such as temperature, pressure, gas velocity etc., the electrical parameters such as electric field and current density, plasma parameters such as electrical conductivity  $\sigma$  and the Hall parameter  $\beta$  are spatially uniform. Also, it is assumed that the ion slip can be ignored and the magnetic field  $B$  consists of only the applied one which is parallel to  $z$ -axis.

To simplify the analysis, let us introduce the new coordinate axes  $X$  and  $Y$  as shown in Fig. 4, corresponding to the slant of any space element, instead of the conventional rectangular coordinate axes  $x$  and  $y$ . Then,

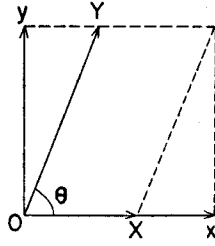


Fig. 4. Old- and new-coordinates.

$$\begin{bmatrix} x \\ y \end{bmatrix} = \begin{bmatrix} 1 & \cos \theta \\ 0 & \sin \theta \end{bmatrix} \begin{bmatrix} X \\ Y \end{bmatrix}. \quad (1)$$

As is well known, the two dimensional Ohm's law in the  $x$ - $y$  coordinate system is written as follows:

$$\left. \begin{aligned} E_x' &= E_x = (J_x + \beta J_y) / \sigma, \\ E_y' &= E_y - uB = (-\beta J_x + J_y) / \sigma, \end{aligned} \right\} \quad (2)$$

where  $E_x'$  and  $E_y'$  are the  $x$ - and  $y$ -components of the electric field in the coordinate system moving with a gas velocity  $u$ ,  $E_x$  and  $E_y$  are the  $x$ - and  $y$ -components of the electrostatic field, and  $J_x$  and  $J_y$  are the same ones of the current density respectively. Using Eq. (1), Eq.s (2) are transformed to the following equations in the  $X$ - $Y$  coordinate system,

$$\left. \begin{aligned} E_X' &= [(1 + \beta \cot \theta) J_X + \beta J_Y \operatorname{cosec} \theta] / \sigma, \\ E_Y' &= [-\beta J_X \operatorname{cosec} \theta + (1 - \beta \cot \theta) J_Y] / \sigma, \end{aligned} \right\} \quad (3)$$

where  $J_X$  and  $J_Y$  are the  $X$ - and  $Y$ -components of the current density and  $E_X'$  and  $E_Y'$  are the same ones of the electric field in the moving coordinate system respectively.

Next, the real voltages  $V_\eta'$  and  $V_\xi'$  in the  $Y$ - and  $X$ -directions between both end surfaces of a space element are given as follows:

$$\left. \begin{aligned} V_\eta' &= - \int_0^{h \operatorname{cosec} \theta} (E_Y' + E_X' \cos \theta) dY = -h \operatorname{cosec} \theta (E_Y' \sin \theta + E_X' \cos \theta) \\ &= -[(\cos \theta - \beta \sin \theta) J_x + (\sin \theta + \beta \cos \theta) J_y] h \operatorname{cosec} \theta / \sigma, \\ V_\xi' &= - \int_0^s E_X \sin^2 \theta dX = -s \cdot \sin^2 \theta (E_x' - E_y' \cot \theta) \\ &= -s \cdot \sin^2 \theta [J_x + \beta J_y - (J_y - \beta J_x) \cot \theta], \end{aligned} \right\} \quad (4)$$

respectively. Also the total net currents  $I_\xi$  and  $I_\eta$  in  $X$ - and  $Y$ -directions and the voltages  $V_\xi$  and  $V_\eta$  in the  $X$ - and  $Y$ -directions between both end surfaces of

the space element are defined as follows:

$$\left. \begin{aligned} I_{\xi} &= d \cdot h \cdot (J_x - J_y \cot \theta), \\ I_{\eta} &= d \cdot s \sin \theta (J_y \sin \theta + J_x \cos \theta), \end{aligned} \right\} \quad (5)$$

$$\left. \begin{aligned} V_{\xi} &= -s \cdot \sin^2 \theta (E_x - E_y \cot \theta), \\ V_{\eta} &= -h(E_y + E_x \cot \theta), \end{aligned} \right\} \quad (6)$$

respectively. By the Eq. (4) to (6), the following relations are derived.

$$\begin{bmatrix} V_{\eta}' \\ V_{\xi}' \end{bmatrix} = \begin{bmatrix} V_{\eta} + huB \\ V_{\xi} - suB \sin \theta \cos \theta \end{bmatrix} = [Z] \begin{bmatrix} -I_{\eta} \\ -I_{\xi} \end{bmatrix}, \quad (7)$$

where

$$\left. \begin{aligned} [Z] &= \begin{bmatrix} R_{\eta} & -R_m \\ R_m & R_{\xi} \end{bmatrix}, \\ R_{\eta} &= h/(d\sigma s \sin^2 \theta), \\ R_{\xi} &= s \sin^2 \theta / (\sigma dh), \\ R_m &= (\beta/\sigma)/d, \end{aligned} \right\} \quad (8)$$

where  $[Z]$ , which we derived by the above mentioned treatment, can be regarded as the equivalent impedance matrix of a space element. Therefore we can exhibit a space element by the equivalent four-terminal circuit as shown in Fig. 5(a).

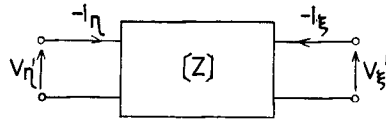


Fig. 5(a). Equivalent four-terminal network for space element.

### 3.2 Fundamental matrix and equivalent four-terminal network

We can rewrite the relation expressed in Eq. (7) as follows:

$$\begin{bmatrix} V_{\eta}' \\ -I_{\eta}' \end{bmatrix} = [F] \begin{bmatrix} V_{\xi} \\ I_{\xi} \end{bmatrix}, \quad (9)$$

with the so-called fundamental matrix  $[F]$ , where

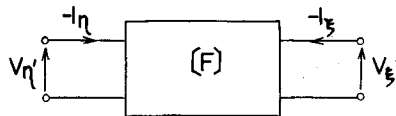


Fig. 5(b). Equivalent four-terminal network for space element.

$$[F] = \begin{bmatrix} A & B \\ C & D \end{bmatrix}, \quad (10)$$

in which

$$\left. \begin{aligned} A &= R_\eta/R_m, & B &= (R_\eta R_\xi - R_m^2)/R_m, \\ C &= 1/R_m, & D &= R_\xi/R_m, \end{aligned} \right\} \quad (11)$$

in which  $A$ ,  $B$ ,  $C$  and  $D$  are the equivalent four-terminal network constants. However from Eq.s (11)

$$\det [F] = -1. \quad (12)$$

Therefore, the equivalent circuit which Eq. (9) represents is not the reciprocal one. Hence the equivalent circuit cannot be composed of only passive elements. It should also contain the gyrator or negative resistance.<sup>1)</sup>

Next the impedance matrix  $[Z]$  can be transformed as follows:

$$[Z] = [Z'] + \begin{bmatrix} -R_m & -R_m \\ -R_m & -R_m \end{bmatrix}, \quad (13)$$

where

$$[Z'] = \begin{bmatrix} R_\eta + R_m & 0 \\ 2R_m & R_\xi + R_m \end{bmatrix}. \quad (14)$$

So, by making use of a negative resistance<sup>1)</sup>, Eq. (13) is expressed by the equivalent circuit as shown in Fig. 5(c).

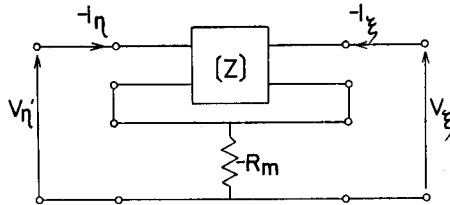


Fig. 5(c). Equivalent four-terminal network for space element.

Again we can derive the fundamental matrix  $[F']$  as follows:

$$\begin{aligned} [F'] &= \begin{bmatrix} (R_\eta + R_m)/(2R_m) & (R_\eta + R_m)(R_\xi + R_m)/(2R_m) \\ 1/(2R_m) & (R_\xi + R_m)/(2R_m) \end{bmatrix} \\ &= \begin{bmatrix} 1 & R_\eta + R_m \\ 0 & 1 \end{bmatrix} \begin{bmatrix} 0 & 0 \\ 1/(2R_m) & 0 \end{bmatrix} \begin{bmatrix} 1 & R_\xi + R_m \\ 0 & 1 \end{bmatrix}, \end{aligned} \quad (15)$$

corresponding to  $[Z']$ . From Eq. (15) and Fig. 5(c), we can acquire the equivalent circuit as shown in Fig. 6. Considering Fig. 6 together with Eq. (7), the space element as shown in Fig. 3 can be expressed by the fundamental equivalent circuit as shown in Fig. 7. Referred to the figure, it is physically forecasted that the electromotive force  $uBh (>0)$  yields the current  $I_\eta (<0)$  and moreover it generates equivalent voltage source  $2R_m I_\eta$  and the current  $I_\xi$ .

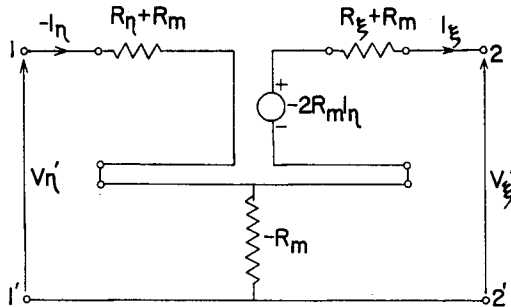


Fig. 6. Equivalent fundamenal circuit for space element.

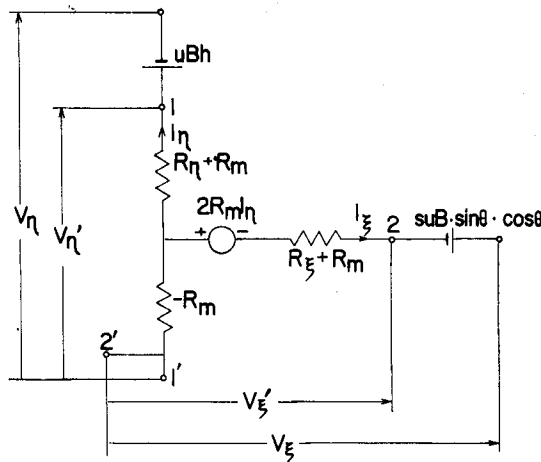


Fig. 7. Equivalent fundamental circuit of space element.

As the duct space is composed of many space elements, the duct is replaced by the connection of many four-terminal circuits.

#### 4. Application of Equivalent Circuit to Multi-Electrode MHD Generators

##### 4.1 Application to the diagonal generator of type I

First, let us apply the above mentioned equivalent circuit to the diagonal



generator of type I. Actually, the space element assumed in Section 3 is a small domain within the duct. The more accurate an analysis is expected, the more space elements the duct space must be divided into, and therefore the more complicated the treatment becomes.

Here, for practical use and simplicity, we divide the space between a pair of electrodes into three space elements, i.e. the anode boundary layer, core flow layer and cathode boundary layer. We shall describe the treatment of the boundary layer in Section 6. The longitudinal length of a space element coincides with the electrode pitch. Also it is assumed that all the parameters in a space element are uniform in  $z$ -direction. Now Fig. 8 shows the equivalent circuit of the space

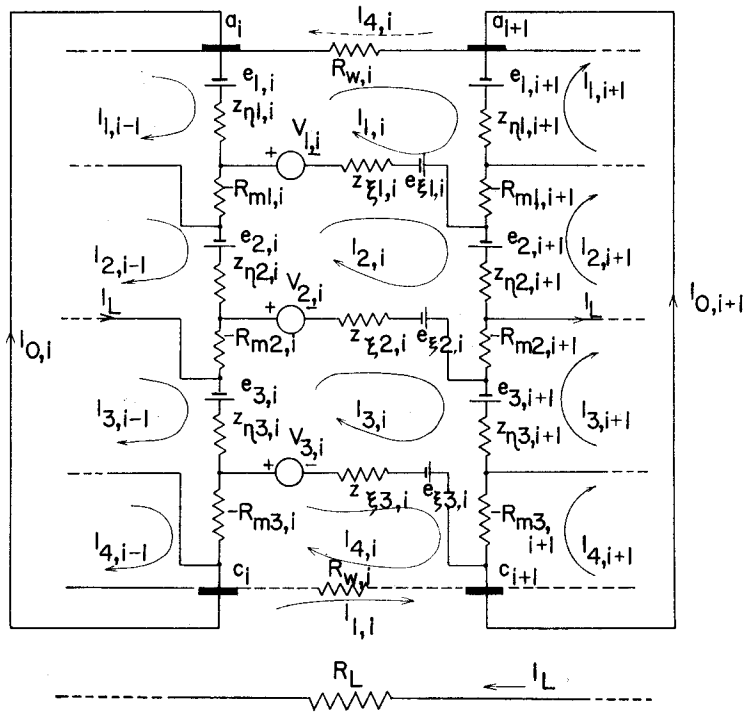


Fig. 8. A part of the equivalent circuit of the duct.

between each pair of electrodes of the diagonal generator duct with the slanted short-circuit electrodes, except the duct inlet- and outlet sections. For simplification of circuit analysis, it is convenient to adopt the mesh currents  $I_{1,i-1}$ ,  $I_{1,i}$ ,  $I_{1,i+1}$  ...etc. as shown in Fig. 8. In this figure,

$$\left. \begin{aligned}
 Z_{\eta j,i} &= R_{\eta j,i} + R_{m j,i}, \\
 Z_{\xi j,i} &= R_{\xi j,i} + R_{m j,i}, \\
 V_{j,i} &= 2R_{m j,i}(I_{j,i} - I_{j,i-1} - I_{0,i}), \\
 R_{\eta j,i} &= h_{j,i} |d \cdot s_i \sin^2 \theta| / \sigma_{j,i}, \\
 R_{\xi j,i} &= s \cdot \sin^2 \theta |dh_{j,i}| / \sigma_{j,i}, \\
 R_{m j,i} &= (1/d)(\beta_{j,i} / \sigma_{j,i}), \\
 e_{j,i} &= h_{j,i} u_{j,i} B, \\
 e_{\xi i,i} &= s_i u_{j,i} B \cos \theta \sin \theta, \\
 \sum_{j=1}^3 h_{j,i} &= H_i, \\
 i &= 1, 2, \dots, n \text{ (number of electrode pair)}, \\
 j &= 1, 2, 3,
 \end{aligned} \right\} \tag{16}$$

and  $R_{w,i}$  is the equivalent wall-leakage resistance between adjacent electrodes. When each pair of electrodes  $a_i$  and  $c_i$  is connected with wire instead of the slanted short-circuit electrode, the separate equivalent leakage resistance should be added between the adjacent anode electrodes and between adjacent cathode electrodes respectively. In this case  $I_{1,i}$  directly does not come in contact with  $I_{4,i}$ .

The network equations for the equivalent circuit in Fig. 8 are as follows:

$$\begin{aligned}
 &(R_{w,i} + R_{\eta 1,i} + R_{\xi 1,i} + R_{\eta 1,i+1})I_{1,i} - (R_{\eta 1,i} - R_{m 1,i})I_{1,i-1} \\
 &- (R_{\eta 1,i+1} + R_{m 1,i+1})I_{1,i+1} - (R_{\xi 1,i} + R_{m 1,i})I_{2,i} + R_{m 1,i+1}I_{2,i+1} \\
 &- R_{w,i}I_{4,i} - (R_{\eta 1,i} - R_{m 1,i})I_{0,i} + R_{\eta 1,i+1}I_{0,i+1} = e_{1,i+1} - e_{1,i} - e_{\xi 1,i}, \tag{17}
 \end{aligned}$$

$$\begin{aligned}
 &- R_{m 1,i}I_{1,i-1} - (R_{\xi 1,i} - R_{m 1,i})I_{1,i} + (R_{\eta 2,i} + R_{\xi 2,i} + R_{\xi 1,i} + R_{\eta 2,i+1})I_{2,i} \\
 &- (R_{\eta 2,i} - R_{m 2,i})I_{2,i-1} - (R_{\eta 2,i+1} + R_{m 2,i+1})I_{2,i+1} - (R_{\xi 2,i} + R_{m 2,i})I_{3,i} \\
 &+ R_{m 2,i+1}I_{3,i+1} - (R_{\eta 2,i} - R_{m 2,i} + R_{m 1,i})I_{0,i} + R_{\eta 2,i+1}I_{0,i+1} \\
 &- (R_{\xi 2,i} + R_{m 2,i} - R_{m 2,i+1})I_L = e_{2,i+1} - e_{2,i} - e_{\xi 2,i} + e_{\xi 1,i}, \tag{18}
 \end{aligned}$$

$$\begin{aligned}
 &- R_{m 2,i}I_{2,i-1} - (R_{\xi 2,i} - R_{m 2,i})I_{2,i} + (R_{\eta 3,i} + R_{\xi 3,i} + R_{\xi 2,i} + R_{\eta 3,i+1})I_{3,i} \\
 &- (R_{\eta 3,i} - R_{m 3,i})I_{3,i-1} - (R_{\eta 3,i+1} + R_{m 3,i+1})I_{3,i+1} - (R_{\xi 3,i} + R_{m 3,i})I_{4,i} \\
 &+ R_{m 3,i+1}I_{4,i+1} - (R_{\eta 3,i} - R_{m 3,i} + R_{m 2,i})I_{0,i} + R_{\eta 3,i+1}I_{0,i+1} \\
 &+ R_{\xi 2,i}I_L = e_{3,i+1} - e_{3,i} - e_{\xi 3,i} + e_{\xi 2,i}, \tag{19}
 \end{aligned}$$

$$-R_{m 3,i}I_{3,i-1} - (R_{\xi 3,i} - R_{m 3,i})I_{3,i} + (R_{w,i} + R_{\xi 3,i})I_{4,i} - R_{m 3,i}I_{0,i} = e_{\xi 3,i}, \tag{20}$$

$$\begin{aligned}
 &R_{\eta 1,i}I_{1,i-1} - (R_{\eta 1,i} + R_{m 1,i})I_{1,i} + R_{\eta 2,i}I_{2,i-1} - (R_{\eta 2,i} + R_{m 2,i} - R_{m 1,i})I_{2,i} \\
 &+ R_{\eta 3,i}I_{3,i-1} - (R_{\eta 3,i} + R_{m 3,i} - R_{m 2,i})I_{3,i} + R_{m 3,i}I_{4,i} \\
 &+ (R_{\eta 1,i} + R_{\eta 2,i} + R_{\eta 3,i})I_{0,i} = e_{1,i} + e_{2,i} + e_{3,i}, \tag{21}
 \end{aligned}$$

$$\begin{aligned}
 &\sum_i \{R_{m 2,i}I_{2,i-1} + (R_{\xi 2,i} - R_{m 2,i})I_{2,i} - R_{\xi 2,i}I_{3,i} \\
 &+ R_{m 2,i}I_{0,i} - R_{\xi 2,i}I_L\} = R_L I_L - \sum_i e_{\xi 2,i}, \tag{22}
 \end{aligned}$$

where  $R_L$  is the load resistance. One may be concerned that the number of the unknown is more than that of the equations, but this phase will be removed when the network for the whole duct is completed. By solving these equations simultaneously, the performance of the diagonal MHD generator is known perfectly.

Next, if the periodicity of the physical quantities is kept between the duct inlet and outlet, namely

$$\left. \begin{aligned} I_{0,i} &= I_{0,i+1} \equiv I_0, \\ I_{j,i-1} &= I_{j,i} = I_{j,i+1} \equiv I_j, \\ e_{j,i} &= e_{j,i+1} \equiv e_j, \\ R_{\eta j,i} &= R_{\eta j,i+1} \equiv R_{\eta j}, \\ R_{\xi j,i} &= R_{\xi j,i+1} \equiv R_{\xi j}, \\ R_{mj,i} &= R_{mj,i+1} \equiv R_{mj}, \\ j &= 1, 2, 3, \end{aligned} \right\} \quad (23)$$

the treatment of Eq.s (17) to (22) is extremely simplified.

Moreover, if each parameters in the anode region is equal to that in the cathode region respectively, i.e.

$$\left. \begin{aligned} e_1 &= e_3 \equiv e_b, & R_{\eta 1} &= R_{\eta 3} \equiv R_{\eta b}, \\ R_{\xi 1} &= R_{\xi 3} \equiv R_{\xi b}, & R_{m 1} &= R_{m 3} \equiv R_{m b}, \end{aligned} \right\} \quad (24)$$

In addition, if the suffix 2 of  $e$ 's and  $R$ 's is replaced by the suffix 0 for convenience, then Eq.s (17) to (22) are simplified as follows:

$$(R_w + R_{\xi b})I_1 - R_{\xi b}I_2 - R_wI_4 + R_{mb}I_0 = -e_{\xi b}, \quad (25)$$

$$-R_{\xi b}I_1 + (R_{\xi b} + R_{\xi 0})I_2 - R_{\xi 0}I_3 - (R_{mb} - R_{m0})I_0 - R_{\xi 0}I_L = -e_{\xi 0} + e_{\xi b} \quad (26)$$

$$-R_{m0}I_2 + (R_{\xi 0} + R_{\xi b})I_3 - R_{\xi b}I_4 - (R_{m0} - R_{mb})I_0 + R_{\xi 0}I_L = -e_{\xi b} + e_{\xi 0} \quad (27)$$

$$-R_{\xi b}I_3 + (R_w + R_{\xi b})I_4 - R_{mb}I_0 = e_{\xi b}, \quad (28)$$

$$\begin{aligned} &-R_{mb}I_1 - (R_{m0} - R_{mb})I_2 - (R_{mb} - R_{m0})I_3 + R_{mb}I_4 + (R_{\eta 0} + 2R_{\eta b})I_0 + R_{m0}I_L \\ &= e_0 + 2e_b, \end{aligned} \quad (29)$$

$$R_{\xi 0}I_2 - R_{\xi 0}I_3 + R_{m0}I_0 - (R_{\xi 0} + R_L')I_L = -e_{\xi 0}, \quad (30)$$

where  $R_L'$  is the equivalent load resistance which may be connected per a pair of electrodes. By solving the Eq.s (25) to (30) simultaneously, the periodical solutions for mesh currents are obtained, and therefore Joule's heat, current density etc. are able to be calculated.

## 4.2 Application to other generators

In the previous article, the authors treated the network equations for the diagonal generator of type I with the slant short-circuit electrodes. As mentioned

in the previous section, the method of our analysis is easily applicable to the generator of type II as well as that of type I, including the Faraday and Hall type of generator. However, there are some differences for each type of generator regarding the equivalent networks and treatments, because there are differences respecting the connection methods of electrodes and load resistances.

In the case of the Hall generator,  $\theta = \pi/2$  and the same technique as in the case of the diagonal generator is used for analyzing the duct performance.

For Faraday generator, similarly  $\theta = \pi/2$  and the load resistance  $R_{L,i}$  must be inserted between the electrodes  $a_i$  and  $c_i$  instead of the short-circuit wire. Therefore, in this case, in Fig. 8  $I_{0,i}$  means the load current, and the load resistance  $R_L$  and load current  $I_L$  must be taken away. Also, the wall-leakage resistance between the adjacent anode electrodes is independent of that of the corresponding adjacent cathode electrodes.

In the case of the diagonal generator of type II, the cathode electrodes  $c_i$  is connected with the anode electrode  $a_{i+1}$  successively, and the load resistance  $R_L$  is connected between  $a_1$  and  $c_n$  (see Fig. 1). Accordingly, in this type of generator, the loop current passes through  $R_L$ ,  $a_1$ ,  $c_1(\equiv a_2)$ , ...,  $c_{n-1}(\equiv a_n)$ ,  $c_n$  and  $R_L$ . The sub-loop current passes through  $c_i(\equiv a_{i+1})$ ,  $c_{i+1}$  and  $c_i$ . Moreover, as well as in the Faraday generator, the wall-leakage resistance in the cathode side is independent of that in the anode side.

### 5. Current Density, Power Loss, Power Output and Electrical Efficiency

#### 5.1 Current density

As is clear from Eq.s (5) and Fig. 7, the current  $I_\xi$  and  $I_\eta$  are the real components of  $\mathbf{J}$  in the  $X$ - and  $Y$ -directions respectively. So we should bear in mind that the vector sum of the current densities  $\mathbf{J}_\xi$  and  $\mathbf{J}_\eta$ , which correspond to  $I_\xi$

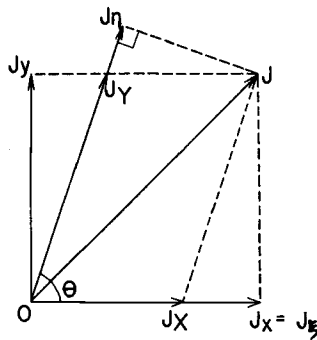


Fig. 9. Relationship among  $\mathbf{J}$  and its various components.

and  $I_\eta$  respectively, does not coincide with the original current density except the case of  $\theta = \pi/2$  (see Fig. 9). When we want to know the direction of current density in a space element, we must seek for the current densities  $J_x$  and  $J_y$ . From Eq.s (5)

$$\left. \begin{aligned} J_x &= I_\xi \sin^2 \theta / d/h + I_\eta \cot \theta / d/s, \\ J_y &= I_\eta / d/s - I_\xi \sin \theta \cos \theta / d/h. \end{aligned} \right\} \quad (31)$$

By similar treatment

$$\left. \begin{aligned} E_x' &= -(V_\xi' / s + V_\eta' \sin \theta \cos \theta / h), \\ E_y' &= -(V_\eta' \sin^2 \theta / h - V_\xi' \cot \theta / s), \end{aligned} \right\} \quad (32)$$

where  $E_\xi'$  and  $E_\eta'$  are respectively the real  $X$ - and  $Y$ -components of the electric field in the coordinate system moving with the gas velocity  $u$ . In the generators of type of  $\theta = \pi/2$  such as the Faraday, Hall and diagonally connected generators, Eq.s (31) and (32) are simplified.

The direction of the current density  $\mathbf{J}$  in a space element can be decided by Eq.s (31). Moreover the distribution of the overall current density in a duct can be known, if  $I_\xi$  and  $I_\eta$  in each equivalent circuit are calculated, since the duct space is composed of many space elements.

## 5.2. Power loss

According to the equivalent circuit in Fig. 7, the electric power

$$\begin{aligned} P_d' &= (R_\eta + R_m) I_\eta^2 + (R_\xi + R_m) I_\xi^2 + 2R_m I_\eta I_\xi - R_m (I_\eta + I_\xi)^2 \\ &= R_\eta I_\eta^2 + R_\xi I_\xi^2, \end{aligned} \quad (33)$$

is dissipated in the circuit. This can be also proved as follows; the power dissipation per unit volume, which means Joule's heat, is calculated by the scalar product of the electric field  $\mathbf{E}'$  and current density  $\mathbf{J}$ , i.e.

$$\mathbf{J} \cdot \mathbf{E}' = J_x E_x' + J_y E_y'. \quad (34)$$

Therefore the power loss  $P_d$  in one space element is

$$P_d = \int_v \mathbf{J} \cdot \mathbf{E}' dv = -(I_\xi V_\xi' + I_\eta V_\eta'), \quad (35)$$

and using Eq.s (7) and (8)

$$P_d = P_d' = R_\eta I_\eta^2 + R_\xi I_\xi^2. \quad (36)$$

In the nonequilibrium generator, this power loss is acted on the elevation of electron temperature.

### 5.3 Power output and electrical efficiency

When we solve Eq.s (17) to (22) simultaneously respecting the whole equivalent circuit and the load current  $I_L$  is found up, then the electrical output power  $P_L$  is

$$P_L = I_L^2 R_L. \tag{37}$$

On the other hand, the generated power in the duct is obtained as follow. In the space element, the motional electromagnetic field  $\mathbf{u} \times \mathbf{B}$  is induced in the negative  $y$ -direction. So using Eq.s (31), the generated electric power  $p_e$  is obtained as follows:

$$\begin{aligned} p_e &= \int_v \mathbf{J} \cdot (\mathbf{u} \times \mathbf{B}) dv = \int_v J_y u B dv = u B J_y dh s \\ &= u B (h I_\eta - s I_\xi \sin \theta \cos \theta). \end{aligned} \tag{38}$$

Accordingly the total power generated in the duct is calculated, for example, for the diagonal generator as shown in Fig. 8 as follows:

$$P_e = \sum_{i=1}^n \sum_{j=1}^3 p_{ej,i}, \tag{39}$$

where

$$p_{ej,i} = u_{j,i} B [h_{j,i} (I_{j,i} - I_{j,i-1} - I_{0,i}) - s (I_{j+1,i} - I_{j,i}) \sin \theta \cos \theta]. \tag{40}$$

Then the electrical efficiency  $\eta_e$  in the generator beomes

$$\eta_e = P_L / P_e = I_L^2 R_L / (\sum_{i=1}^n \sum_{j=1}^3 p_{ej,i}). \tag{41}$$

## 6. Boundary Layer

In the analysis of the gas flow, it may be divided into two parts, i.e. the inviscid core flow and the boundary layer in the vicinity of the duct walls. It is thought that a turbulent flow will be fully developed in the boundary layer. However the boundary layer theory in an MHD duct has not been established completely. Therefore, here let us apply Schlichting's boundary layer theory<sup>5)</sup> on a flat plate to the duct as well as in Ref. 4 (see Fig. 10).

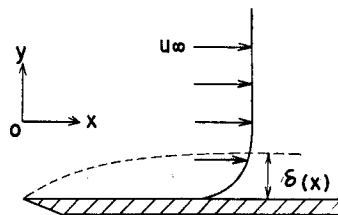


Fig. 10. Boundary layer model of flat plate.

In the analysis, when it is assumed that the viscous and thermal boundary layers have nearly the same thickness, the thickness  $\delta(x)$  is given by

$$\delta(x) = 0.37 \cdot x \cdot R_{ex}(x)^{-0.2}. \quad (42)$$

In this equation,  $R_{ex}(x)$  is the local Reynolds number, which is expressed by

$$R_{ex}(x) = u_\infty \rho x / \mu, \quad (43)$$

in which  $u_\infty$ ,  $\rho$  and  $\mu$  are the core flow velocity, the mass density and the viscosity coefficient respectively, and

$$\mu = 0.195 \times 10^{-6} \cdot T^{0.75} \quad (44)$$

For example, the boundary layer thickness at the distance  $x=L/2$  in the typical experimental scale generator ( $H=0.15$  m,  $L=1$  m,  $u=800$  m/s,  $\rho=0.3$  kg/m<sup>3</sup>,  $T=2500^\circ\text{K}$ ) is equal to about 0.01 m. In the large scale generator ( $H=1.5$  m,  $L=10$  m, other parameters being the same as in the above example), it is equal to about 0.06 m at the distance  $x=L/2$ . In the latter the influence of the boundary layer is quite small. However, it must not be ignored when the behavior of the generator is considered.

When the Prandtl number is nearly equal to 1 and the pressure gradient in the  $x$ -direction can be neglected, the gas velocity distribution in the  $y$ -direction in the boundary layer is given by

$$u/u_\infty = (h_s - h_w)/(h_\infty - h_w) = (y/\delta)^{1/\gamma}, \quad (45)$$

where  $h_s$ ,  $h_w$  and  $h_\infty$  denote the stagnation enthalpy of the boundary layer, on the wall and in the gas core respectively. Then the temperature profile in the layer is determined by the following equation

$$T/T_\infty = T_w/T_\infty + (1 - T_w/T_\infty)u/u_\infty + [(\gamma - 1)/2]M^2(1 - u/u_\infty)u/u_\infty, \quad (46)$$

where  $\gamma$  is the specific heat ratio, and  $T$ ,  $T_w$  and  $T_\infty$  are the temperature of the layer, on the wall and in the gas core respectively. The third term of the right side of Eq. (46) may be neglected in the subsonic region, i.e.

$$T/T_\infty = T_w/T_\infty + (1 - T_w/T_\infty) \cdot u/u_\infty. \quad (47)$$

When the value of  $T_w/T_\infty$  is known, the temperature profile is obtained from Eq.s (45) and (47).

On the other hand, the conductivity  $\sigma$  and the Hall parameter  $\beta$  are generally the functions of the temperature  $T$  and pressure  $p$ . When it is assumed that  $\sigma$  and  $\beta$  are expressed by

$$\left. \begin{aligned} \sigma &= c p^m T^n, \\ \beta &= c' p^{m'} T^{n'} \end{aligned} \right\} \quad (48)$$

in the core flow and the boundary layer, with respect to the latter we obtain

$$\left. \begin{aligned} \sigma/\sigma_\infty &= (T/T_\infty)^n, \\ \beta/\beta_\infty &= (T/T_\infty)^{n'}, \end{aligned} \right\} \quad (49)$$

where  $\sigma_\infty$  and  $\beta_\infty$  are the conductivity and the the Hall parameter in the core flow respectively to be obtained from Eq.s (47) and (49).

Since  $u$ ,  $T$ ,  $\sigma$ ,  $\beta$  etc. vary spacially and dramatically in the  $y$ -direction in the boundary layer, the-boundary layer space must be divided into many space elements if an accurate analysis for that region is wanted. However, as mentioned above, in the large scale generator the thickness of the layer is very thin in comparison to that of the core flow, and consequently the average values  $\langle u \rangle$ ,  $\langle \sigma \rangle$  and  $\langle \beta \rangle$ , i.e.

$$\langle u \rangle = (1/\delta) \int_0^\delta u dy = (7/8)u. \quad (50)$$

$$\langle \sigma \rangle = \sigma_\infty \int_0^1 [T_w/T_\infty + \{1 - (T_w/T_\infty)\} (y/\delta)^{1/n}]^n d(y/\delta), \quad (51)$$

$$\langle \beta \rangle = \beta_\infty \int_0^1 [T_w/T_\infty + \{1 - (T_w/T_\infty)\} (y/\delta)^{1/n'}]^{n'} d(y/\delta), \quad (52)$$

are thought to play fairly well the substitutes of the parameters  $u$ ,  $\sigma$  and  $\beta$  for the analysis of the generator performance.

## 7. Conclusion

(1) The authors pointed out that any MHD generator duct is generally expressed by the combination of many fundamental equivalent four-terminal circuits by introducing the new coordinate axes going to the directions of the gas flow and the electrode pair.

(2) A fundamental equivalent four-terminal circuit was derived from a space element assumed in a duct, using the equivalent negative resistance which originated from the two dimensional Ohm's law.

(3) Considering the leakage current in a duct wall, the application of the fundamental equivalent circuit to the multi-electrode generators, especially the diagonal generator, was attempted. Also, there was reference to the treatment of the Hall, Faraday and diagonally connected generators.

(4) The method to calculate the characteristics of the generator, such as current density, Joule's heat, generated and output powers, electrical efficiency etc. was derived.



(5) The treatment of boundary layer in the duct was discussed.

Lastly, the above mentioned theoretical analysis can very well simulate the performance of the MHD generator, when the duct scale, plasma property and distribution of pressure and temperature in a duct are given.

#### References

- 1) H. Shirakata; Japanese J. of Appl. Phys., **11**, No. 12, 1837-1850 (1972).
- 2) Z. Celinski; Rozprawy Elektrotech., **17**, 1, 109-123 (1971).
- 3) Z. Celinski; Energy Conversion, **10**, 105-112 (1970).
- 4) Z. Celinski; Archiwum Elektrotech., 769-785 (1970).
- 5) H. Schlichting; "Boundary Layer Theory", McGraw Hill, New York (1968).